Effect of Speed Ratio on Surface Finish using Circumferentially-Grooved Vitrified Bond Wheels in Cylindrical Plunge Grinding

Scott Dewar[1, a *], Andrew Warkentin[1,b], and Robert Bauer[1,c*]

[1]Department of Mechanical Engineering, Dalhousie University, Halifax, Canada

[a] scottdewar@dal.ca, [b]andrew.warkentin@dal.ca, [c*]robert.bauer@dal.ca

Keywords: cylindrical grinding, circumferentially-grooved wheel, speed ratio

Abstract. Cutting a single spiral (circumferential) groove into a vitrified bond grinding wheel has been shown to significantly reduce forces, spindle power and cycle time in cylindrical plunge grinding while increasing surface roughness. This paper investigates for the first time the effect of cylindrical-grinding speed ratio on the resulting workpiece surface finish when using circumferentially-grooved grinding wheels. The grooved wheels used in this research have a 50% groove factor (corresponding to the ratio of the grooved portion to the ungrooved portion on the wheel surface). Grinding experiments were carried out using both integer and non-integer speed ratios and the effects on surface roughness were observed. The results showed that integer speed ratios using a circumferentially-grooved wheel can produce thread-like textures on the workpiece which increases the surface roughness. Non-integer speed ratios, however, did not create such a texture and resulted in improved surface roughness. In fact, preliminary results suggest that that a grooved wheel in combination with an optimal speed ratio may be capable of producing the same surface roughness as a non-grooved wheel with reduced cutting forces, spindle power and cycle time.

Introduction

Grooved wheels are grinding wheels that have grooves formed on their working surface. Grooved vitrified bond wheels have been shown to be effective for reducing grinding forces and power in multiple instances [1,2]. These improvements are likely due to improved cutting mechanics and coolant transport through the grinding zone [3]. Cutting mechanics is improved because the cutting edges on the grooves' trailing edge act like a roughing cutter efficiently removing large chips from the workpiece. Coolant transport is also improved because the grooves fill with coolant and carry it into the grinding zone. Unfortunately, many researchers have observed a degradation in surface finish accompanying the reductions in force and power [4-16], while fewer researchers have reported an improvement in surface finish [17,18]. In this paper preliminary research is presented that suggests that the selection of appropriate speed ratios may help explain the mixed surface finish results and that optimizing the speed ratio in cylindrical plunge grinding may mitigate the surface finish problems associated with grooved wheels.

Experiments

To investigate the effect of speed ratio on the surface finish using circumferentially-grooved wheels in cylindrical grinding, a series of grinding experiments were carried out using a Blohm Planomat surface grinder with a custom rotary axis attachment [6]. Cimtech 310 having a concentration of 5.1% was applied to the grinding zone via a coherent jet. The wheel speed and diameter were 1000 rpm and 385 mm, respectively. A single-point diamond dresser was used to inscribe a 101.6 μm deep and 884 μm wide circumferential groove on the 25.4 mm wide grinding wheel to yield a 50% groove factor and a helix angle of 89.92 deg. Plunge grinding experiments were carried out at an infeed rate of 1.27 μm/rev to a depth of cut of 76.2 μm with a dwell time of 5s at this depth. Wheel-to-workpiece angular speed ratios of 4.00, 4.50, 4.76, 4.88 and 5.0 were tested by varying the workpiece speed between 250 and 200 rpm. To provide a point of reference for comparison a plunge grinding experiment was also carried out for a conventional non-grooved wheel at a speed ratio of 4.50.

Results and Discussion

It was observed that integer speed ratios resulted in thread-like surface patterns on the workpiece similar to the ones observed by Oliveira et al. [10,11], while non-integer speed ratios did not exhibit any patterns on the workpiece. Sample workpiece surfaces are shown in Figure 1 for angular speed ratios r_w of 4.00, 4.76 and 5.00. Integer speed ratio cases are discussed first, after which non-integer speed ratios will be discussed.

The thread-like pattern observed for integer speed ratios in Figure 1a) and c) can be explained using Figure 2. In this figure, section views of cylindrical plunge grinding with speed ratios of one, two and three are shown for a grinding wheel with a 50% groove factor for one revolution of the workpiece during the dwell stage (where there is no infeed). The grooved grinding wheels are shown at the top of Figure 2 where the grooved section does not interact with the workpiece and the leading edge of the groove starts at top-dead center on the workpiece. In the case of a speed ratio of one (where the angular velocity of the wheel w_s equals the angular velocity of the workpiece w_w), a cutting edge on the grinding wheel surface will return to the same location on the workpiece once every grinding wheel revolution. Since only half the grinding wheel has cutting edges and every cutting edge will cut in the same location on the workpiece, one section of the workpiece surface will remain uncut as seen in Figure 2a). When the speed ratio is two, then two rotations of the grinding wheel are required for a cutting edge to return to the same position on the workpiece (top-dead center). In this case, two sections of the workpiece will remain uncut as seen in Figure 2b). Similarly, when the speed ratio is three, a total of three rotations of the grinding wheel are required to return to top-dead center resulting in three uncut sections on the workpiece. These uncut sections form the thread-like pattern observed in Figure 1a) and c). During plunge grinding, the grinding wheel will rotate over the same location on the workpiece many times and the uncut sections of the workpiece observed in Figure 2 result in the distinctive thread like patterns observed in the images shown in Figure 1a) and 1c).

The angle of the thread pattern α can be calculated knowing the groove factor η, groove width b_g, and the speed ratio r_w using the geometry shown in Figure 3, where d_s and d_w correspond to the wheel and workpiece diameters, respectively. In this figure the surface of the grinding wheel and workpiece have been unrolled and presented side-by-side. According to Mohamed et al. [19] the groove lead f_g is given by:

$$f_g = \frac{b_g}{\eta} \tag{1}$$

During one revolution of the grinding wheel, the workpiece will revolve a distance D of:

$$D = \frac{\pi d_w}{r_w} \tag{2}$$

Therefore, referring to Figure 3 and Equations (1) and (2), the pattern angle α will be:

$$\alpha = \tan^{-1}\left(\frac{f_g r_w}{\pi d_w}\right) \tag{3}$$

Performing this calculation, the pattern angle on the workpiece shown in Figure 1a) is predicted to be 5.1º when the speed ratio is four, while the pattern angle on the workpiece shown in Figure 1c) is predicted to be 6.3º when the speed ratio is five. These calculations compare reasonably well with the 5º and 6º values directly measured from the workpiece images.

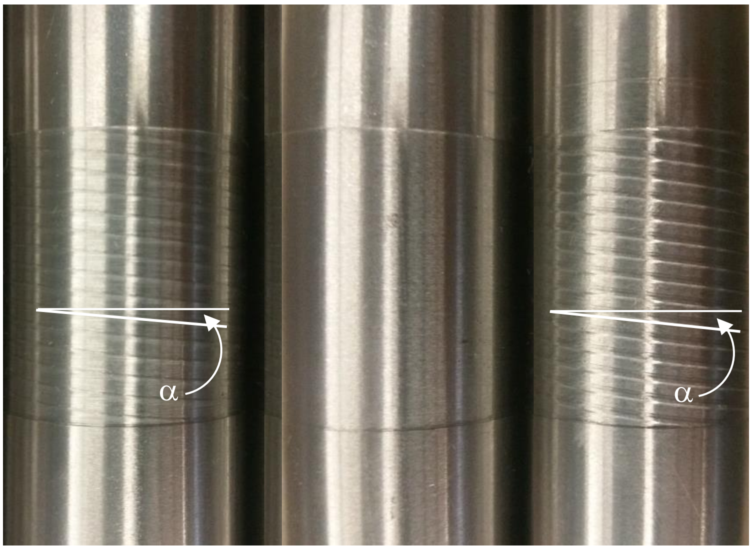

(a) $r_w = 4.00$, $\alpha = 5º$ (b) $r_w = 4.76$ (c) $r_w = 5.00$, $\alpha = 6°$

Figure 1: Sample workpieces

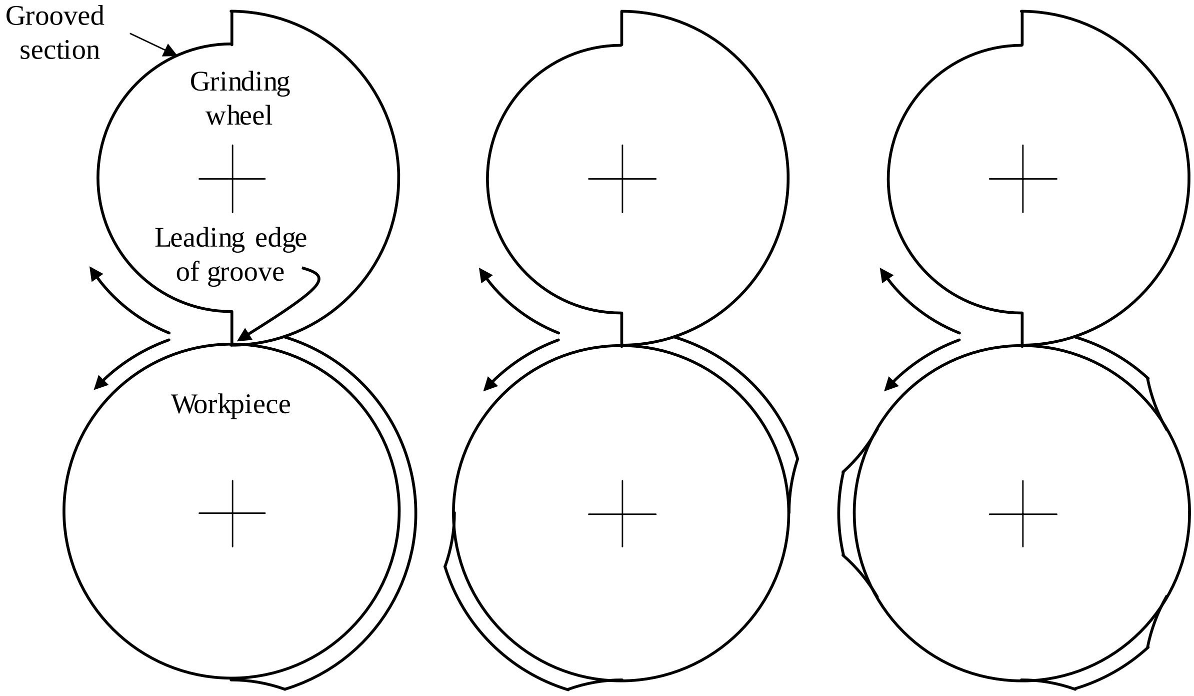

(a) $\omega_s = \omega_w$ (b) $\omega_s = 2\omega_w$ (c) $\omega_s = 3\omega_w$

Figure 2: Effect of integer speed ratio on workpiece surface pattern

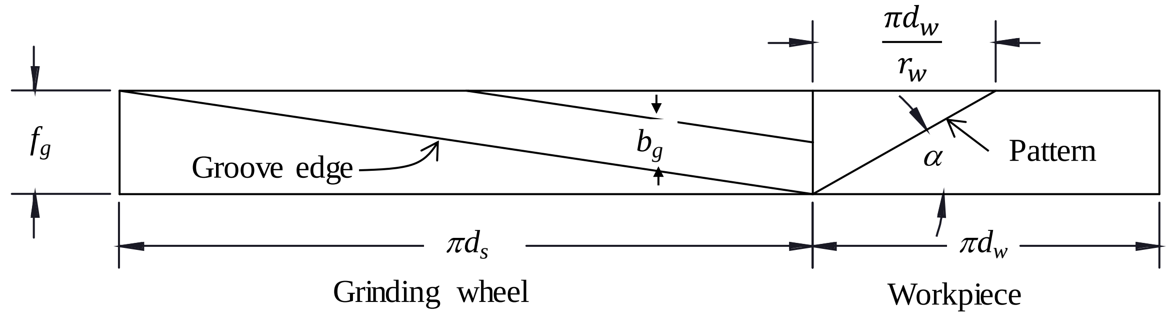

Figure 3: Groove Geometry

The reason why non-integer speed ratios did not produce a thread-like pattern can be explained using Figure 4. This figure shows workpiece section views of cylindrical plunge grinding with a speed ratio of 1.1 during the dwell stage. The evolution of the resulting workpiece surface is shown from left to right each time the grooved grinding wheel makes one complete revolution. Unlike the case when the speed ratio is one, every time the grinding wheel makes one revolution it does not return to top-dead center; rather, the grinding wheel completes its revolution before the workpiece returns to top-dead center and begins to cut unground workpiece material. Over the course of several revolutions of the grinding wheel, the entire workpiece surface becomes cut. It should be noted that the dwell time, speed ratio, workpiece and grinding wheel diameters will influence the number of revolutions of the wheel that are required to completely cut the entire workpiece surface. For example, referring to Figure 4, after six wheel revolutions there is still a small cusp left on the workpiece surface which may not be visible as a surface pattern but could degrade the surface roughness measurements.

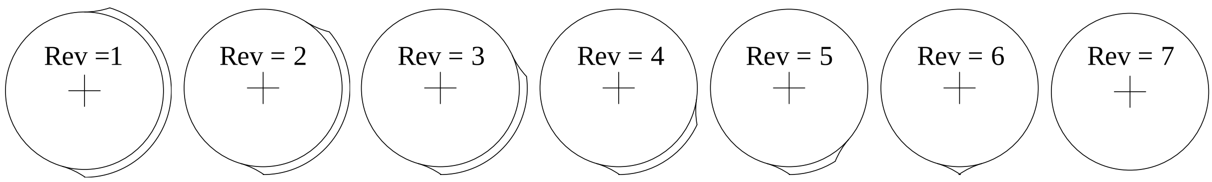

Figure 4: Effect of non-integer speed ratio on workpiece surface pattern

Our preliminary grooved-wheel experimental results showed that, for speed ratios of 4.5, 4.76 and 4.87, the resulting workpiece surface roughness R_a was 0.45, 0.418 and 0.388μm, respectively. The surface roughness of 0.388μm using a grooved grinding wheel with a speed ratio of 4.87 compared well with the surface roughness of 0.374μm using a conventional non-grooved grinding with a speed ratio of 4.5. Based on these results, it is likely that optimal speed ratios exist that will minimize the number of wheel revolutions required to remove workpiece material and perhaps minimize the surface roughness of the resulting workpiece. These results may also help explain the inconsistencies in surface roughness observed in the literature when cylindrical grinding with grooved wheels.

Summary

It was observed in this work that speed ratio plays an important role when cylindrical grinding with circumferentially-grooved grinding wheels. In the case of integer speed ratios, a thread-like texture is created on the workpiece which effectively increases the surface roughness. When non-integer speed ratios are used, however, the resulting workpiece surface becomes smoother with no apparent texture. Preliminary results suggest that optimal non-integer speed ratios may exist that minimize the number of wheel revolutions required to completely remove workpiece material and possibly enable grooved grinding wheels to achieve workpiece surface finishes comparable to conventional non-grooved wheels.

References

1. Li HN, Axinte D (2016) Textured Grinding Wheels: A Review, International Journal of Machine Tools and Manufacturing, 109:8-35
2. Forbrigger C, Bauer R, Warkentin A (2017) A Review of State-of-the-Art Vitrified Bond Grinding Wheel Grooving Processes, The International Journal of Advanced Manufacturing Technology, 90:2207-2216
3. Mohamed A, Bauer R, Warkentin A (2016) Uncut Chip Thickness and Coolant Delivery Effects on the Performance of Circumferentially Grooved Grinding Wheels, The International Journal of Advanced Manufacturing Technology, 85:1429-1438
4. Mohamed AO, Bauer R, Warkentin A (2013) Application of Shallow Circumferential Grooved Wheels to Creep-feed Grinding, Journal of Material Processing Technology, 213:700-706
5. Mohamed A, Bauer R, Warkentin A (2014) A Novel Method for Grooving and Re-grooving Aluminum Oxide Grinding Wheels, The International Journal of Advanced Manufacturing Technology, 73:715-725
6. Dewar S Bauer R Warkentin A (2018) Application of High-angle Helical-grooved Vitrified Wheels to Cylindrical Plunge Grinding, The International Journal of Advanced Manufacturing Technology, 96:2443–2453
7. Nakayama K, Takagi J, Abe T (1977) Grinding Wheel with Helical Grooves - An Attempt to Improve the Grinding Performance, CIRP Annals Manufacturing Technology, 26:133-138
8. Verkerk J (1979) Slotted Wheels to Avoid Cracks in Precision Grinding, Presented at Abrasive Engineering Society Conference. 75-81.
9. Kwak J, Ha M (2001) Force Modeling and Machining Characteristics of the Intermittent Grinding Wheels, Journal of Mechanical Science and Technology, 15:351-356
10. da Silva E, de Oliveira J, Salles B, Cardoso R, Reis V (2013) Strategies for Production of Parts Textured by Grinding using Patterned Wheels, CIRP Annals Manufacturing Technology, 62:355-358
11. Oliveira JFG, Bottene AC, França TV (2010) A Novel Dressing Technique for Texturing of Ground Surfaces, CIRP Annals Manufacturing Technology, 59:361-364
12. Babu NR, Radhakrishnan V (1989) Investigations on Laser Dressing of Grinding Wheels—Part II: Grinding Performance of a Laser Dressed Aluminum Oxide Wheel, Journal of Engineering for Industry, 111:253-261
13. Phanindranath V, Babu NR (1996) A Theoretical Model for Prediction of Groove Geometry on Laser Dressed Grinding Wheel Surface, International Journal of Machine Tools and Manufacturing. 36:1-16

14. Babu NR, Radhakrishnan V, Murti YVGS (1989) Investigations on Laser Dressing of Grinding Wheels—Part I: Preliminary Study, Journal of Engineering for Industry, 111:244-252
15. Denkena B, Grove T, Gottsching T (2015) Grinding with Patterned Grinding Wheels, CIRP Journal of Manufacturing Science and Technology, 8:12-21
16. Kim J, Kang Y, Jin D, Lee Y (1997) Development of Discontinuous Grinding Wheel with Multi-porous Grooves, International Journal of Machine Tools and Manufacturing, 37:1611-1624
17. Köklü U (2012) Grinding with Helically Grooved Wheels, Proceedings of the Institution of Mechanical Engineers, Part E: Journal of Process Mechanical Engineering, 228:33-42
18. Uhlmann E, Hochschild L (2013) Tool Optimization for High Speed Grinding, Production Engineer, 7:185-193
19. Mohamed A, Warkentin A, Bauer R (2016) Prediction of Workpiece Surface Texture Using Circumferentially Grooved Grinding Wheels, The International Journal of Advanced Manufacturing Technology, 89:1149-1160